Electrostatic Interactions with Choline and Phosphate Groups Regulate Cisplatin Permeation through a Dioleoylphosphocholine Bilayer

Lorena Ruano,[a] *Gustavo Cardenas,*[a] *and Juan J. Nogueira*[a,b,*]

[a]Chemistry Department, Universidad Autónoma de Madrid, Calle Francisco Tomás y Valiente, 7, 28049 Madrid, Spain.

[b]IADCHEM, Institute for Advanced Research in Chemistry, Universidad Autónoma de Madrid, Calle Francisco Tomás y Valiente, 7, 28049 Madrid.

KEYWORDS. Cisplatin, Lipid Bilayer, Permeation, Umbrella Sampling, Molecular Dynamics.

ABSTRACT. The investigation of the intermolecular interactions between platinum-based anticancer drugs and lipid bilayers is of special relevance to unveil the mechanisms involved in different steps of the mode of action of these drugs. We have simulated the permeation of cisplatin through a model membrane composed of 1,2-dioleoyl-sn-glycero-3-phosphocholine lipids by means of umbrella sampling classical molecular dynamics simulations. The initial physisorption of cisplatin in the polar region of the membrane is controlled, in a first moment, by long-range electrostatic interactions with the choline groups, which trap the drug in a shallow free-energy minimum. Then, cisplatin is driven to a deeper free-energy minimum by long-range electrostatic interactions with the phosphate groups. From this minimum to the middle of the bilayer the electrostatic repulsion between cisplatin and the choline groups partially cancels out the electrostatic attraction between cisplatin and the phosphate groups, inducing a general drop of the total interaction with the polar heads. In addition, the attractive interactions with the non-polar tails, which are dominated by van der Waals contributions, gain significance. The large energy barrier found when going from the global minimum to the middle of the membrane indicates that the non-electrostatic interactions between the drug and the non-polar tails are badly reproduced by the fixed point-charge force field used here, and that the introduction of polarization effects are likely necessary.

INTRODUCTION

The biological activity of cis-diamminedichloroplatinum (II) (cisplatin) was accidentally discovered in 1965 while investigating the role of electromagnetic radiation in bacterial cell division.[1] Subsequent tests in mice bearing sarcoma and leukemia showed remarkable tumor regression after administration of cisplatin and other platinum complexes.[2] The first clinical tests in patients were conducted in 1971 and just seven years later cisplatin was approved by the U.S. Food and Drug Administration.[3, 4] Since then, an impressive amount of experimental[3, 5-11] and theoretical[12-17] work has been carried out to elucidate the mechanism of action of cisplatin, which is widely employed as chemotherapeutic drug in the treatment of patients with bladder, ovarian, head and neck, lung, testicular, cervical, esophageal, breast and brain cancers.[18] Moreover, the success shown by cisplatin motivates the design and investigation of many other platinum-based compounds with improved biophysiological properties in the last decades.[19-25]

The first step of the mode of action of cisplatin and related compounds is the entry of the drug in the cancer cells. This occurs by passive diffusion through the cell membrane and by facilitated transporters, such as the CTR1 copper transport protein.[9, 26] Despite its hydrophilic nature, permeability assays have shown that cisplatin is able to diffuse through the lipid bilayer due to its small size and neutral charge.[27] Once in the cytosol, cisplatin is activated by the hydrolysis of the Pt-Cl bonds, in which one or two chloride ligands are replaced by water to form the mono-aqua $[Pt(NH_3)_2(OH_2)Cl]^+$ or the diaqua $[Pt(NH_3)_2(OH_2)_2]^{2+}$ platinum complexes.[28] The dissociation of the chloride ligands is favored inside the cell due to the low chloride ion concentration, which is around 13 times lower than in the extracellular fluid.[27] After hydrolysis, the cationic platinum species are able to enter the cell nucleus and react with nucleophilic molecules, *e.g.*, DNA strands. Specifically, the platinum atom of the hydrolyzed drug undergoes a nucleophilic attack

by the N7 atoms of the purine bases, especially guanine, to form different types of DNA lesions, including monoadducts, intrastrand crosslinks and interstrand crosslinks.[4, 7] The most common DNA damage is given by the formation of 1,2-d(GpG) intrastrand crosslinks and, to a lesser extent, 1,2-d(ApG) intrastrand crosslinks, where cisplatin binds to two adjacent guanine nucleobases or to a adenine-guanine stacked pair, respectively. The formation of adducts between DNA and cisplatin – or other platinum complexes – induces structural distortions in the DNA helix. These helical alterations are recognized by several cellular proteins, which can initiate different complex cellular processes, including programmed cell death or apoptosis.[4, 7, 29]

One of the key steps in the mode of action of cisplatin is the transport of the drug across the membrane of the tumor cells. In fact, one possible mechanism by which cancer cells develop resistance to the chemotherapy treatment is a reduced accumulation of cisplatin, in which different cell-membrane processes are involved.[7, 27, 30] In some cancer cells, the membrane-related resistance pathways are more important than the DNA-related ones and may represent 90% of total resistance.[29] A reduced drug accumulation may be caused either by a decrease in drug uptake or by an increase in drug efflux. The passive permeation of the drug through the bilayer depends on several factors. For example, molecular dynamics simulations have evidenced that the lipid composition, the cholesterol content and the curvature of the membrane drastically affect the permeation of cisplatin.[16, 17] Membrane fluidity also plays a relevant role in the passive diffusion mechanism; it has been suggested that a decrease in membrane fluidity hampers the entry of cisplatin into the cells.[31] The fluidity of the bilayers depends, among other factors, on the insertion of molecules into the bilayer and the interactions between those molecules and the lipids.[9] Atomic force microscopy experiments have revealed that cisplatin-encapsulated liposomes are significantly stiffer and more stable than cisplatin-free liposomes.[32]

Therefore, it could be hypothesized that the presence of cisplatin into the membrane might affect its own diffusion and uptake efficacy.

The interaction between cisplatin and membrane rafts, which can induce changes in the biophysical properties of the membrane, is not only involved in resistance mechanisms but also in different apoptotic routes.[9, 33] Although it was generally assumed that cisplatin-induced apoptosis occurs mainly through DNA adduct formation, the consideration exclusively of these DNA-mediated pathways is not enough to explain the toxicity exerted by cisplatin,[33,34] and other mechanisms have to be invoked, including those where the lipid membrane plays a central role. Drug-lipid interactions are also relevant in the liposomal formulations of the drugs aimed to enhance the control over the delivery process and to reduce side effects and resistance of the anticancer compounds.[34] The encapsulation of drugs inside vesicular lipid bilayers facilitates the transport of both hydrophilic and hydrophobic species, which are integrated in the polar and in the lipophilic region of the vesicle, respectively. The liposomal formulation of cisplatin, called lipoplatin, has been successfully developed and administered in clinical trials showing lower side effects than cisplatin.[35] One possible mechanism for the delivery of the encapsulated cisplatin is the fusion of the membrane of the transport vesicle with the membrane of the cancer cell followed by the release of the drug. The efficiency of this process is largely regulated by the interactions between cisplatin and the lipids of both the carrier and the target cell.

Since cisplatin/lipid interactions play a decisive role in the initiation of apoptotic routes, resistance mechanisms and delivery of the drug from liposomal carriers, the rigorous characterization of these interactions is a necessary step towards a comprehensive understanding of the role played by lipid membranes in the mode of action of cisplatin and related species. In the present study, we unveil the intermolecular interactions that regulate the integration of

cisplatin inside a model membrane composed of 1,2-dioleoyl-sn-glycero-3-phosphocholine (DOPC) lipids by means of umbrella sampling classical molecular dynamics simulations. The DOPC membrane was chosen as a model because phosphatidylcholine is one of the major phospholipids components of the plasma membrane and in the membrane of endoplasmic reticulum, Golgi apparatus, mitochondria, endosomes and lysosomes.[36] It has been recently stated that a single-component DOPC membrane does not reproduce with accuracy the features of cisplatin permeation into more realistic cell membranes.[16] However, a detailed analysis of cisplatin/membrane interactions has never been performed even for such a simplified membrane model. Therefore, the investigation presented here is an inescapable step before tackling an analysis of the interactions between cisplatin and more complex bilayers. In addition, the use of simplified models facilitates the evaluation of the theoretical methods employed in the simulations, *e.g.*, the accuracy of the force field.

COMPUTATIONAL METHODS

The lipid bilayer formed by 144 molecules of DOPC per layer with a 25 Å of water thickness on each side was built with the help of the CHARMM-GUI website.[37] Furthermore, a concentration of 0.15 M of KCl was added to reproduce the physiological concentration of this salt. Then, cisplatin was manually placed at a distance of 35 Å from the centre of mass of the membrane using the *tleap* module of AmberTools19,[38] resulting in a system of 34535 atoms. The lipid bilayer was described by the Lipid17 force field, which is an update of the previously developed Lipid11[39] and Lipid14[40] force fields for lipids. Water molecules were described by the TIP3P model[41] and the K^+ and Cl^- ions by suitable Amber parameters.[42] The bond, angle and dihedral

parameters of cisplatin were obtained using the *MCPB.py* module[43] of AmberTools19,[38] whereas the restrained electrostatic potential charges of cisplatin were calculated by B3LYP using the LANL2DZ effective core potential for the platinum atom and the 6-31G* basis set for the other atoms. The charges were computed for the geometry optimized at the same level of theory, using the Gaussian16 software.[44] The Lennard-Jones parameters for the platinum atom were taken from a previous parameterization[45] of metal cations in oxidation state II, which were developed to reproduce the experimental properties, including hydration free energies and coordination numbers. The Lennard-Jones parameters for the rest of the cisplatin atoms were taken from the general Amber force field.[46] All the simulations described below have been evolved by the *pmemd* CUDA implementation[47] of the Amber18 program.[38]

Once the system was set up, the following step was to equilibrate the structure and the density of the solvated bilayer. At first, the whole system was minimized using the steepest descent method for 5000 steps, and the conjugate gradient method for another 5000 steps. Then, it was gradually heated in the canonical (NVT) ensemble, employing a Langevin thermostat with a collision frequency of 1 ps^{-1}, to 300 K for 300 ps. Positional restraints were imposed on the lipid bilayer and on the cisplatin molecule during the heating process, by applying force constants of 10 kcal/(mol$Å^2$) and 5 kcal/(mol$Å^2$), respectively. Once the system was at 300 K, three consecutive molecular dynamics simulations of 4 ns each were performed at constant pressure (isothermal-isobaric NPT ensemble), in which the positional restraints on the lipid were gradually decreased by applying force constants of 10 kcal/(mol$Å^2$), 5 kcal/(mol$Å^2$) and 0 kcal/(mol$Å^2$), correspondingly, whereas the force constant of 5 kcal/(mol$Å^2$) applied on the cisplatin molecule was kept throughout the three NPT simulations. The Berendsen barostat with a pressure relaxation time of 1 ps was employed to maintain the pressure around 1 bar. Finally, a 100 ns

production simulation was performed in the NPT ensemble where the restrain force constant of the cisplatin was maintained at 5 kcal/(molÅ^2). For all the steps of this protocol the Particle Mesh Ewald method[48] was used to calculate the Coulomb interactions, where the direct-space sum was limited to a cutoff of 10 Å. For the computation of van der Waals interactions the same cutoff was applied. In addition, bond distances involving H atoms were restrained by using the SHAKE algorithm[49] and a time step of 2 fs was employed.

After the equilibration of the system, the permeation of cisplatin through the DOPC lipid bilayer was simulated by umbrella sampling molecular dynamics. The reaction coordinate was defined as the distance between the centre of mass of cisplatin and the centre of mass of the membrane along the z axis (normal to the membrane), as schematically shown in Figure 1A. The initial value of the reaction coordinate was 34.5 Å. This distance was divided into 69 windows separated by 0.5 Å. A molecular dynamics simulation of 15 ns was carried out at constant pressure (NPT) on each of the windows applying a harmonic bias potential with a force constant of 5 kcal/(molÅ^2) on the reaction coordinate. Therefore, a total time of 1035 ns was run to simulate the permeation of cisplatin. These simulations were performed sequentially, *i.e.*, the initial conditions (geometry and velocities) of a window were selected from the last snapshot of the previous window. The same technical parameters employed for the 100 ns production described above were used in the simulation of each window. The free-energy profile was obtained by means of the Weighted Histogram Analysis Method (WHAM).[50, 51] The energy-decomposition and the interaction-energy analyses were performed using the *cpptraj* module[52] of the AmberTools19 suite.[38] Visual Molecular Dynamics[53] was used to visualize the trajectories.

RESULTS AND DISCUSSION

Equilibration and Umbrella Sampling Setup

The diffusion of cisplatin through a lipid DOPC bilayer has been simulated by umbrella sampling molecular dynamics simulations. This enhanced-sampling approach is widely employed for modelling the slow diffusion process of small molecules across membranes[16, 17, 54-56] because it allows an efficient sampling along the permeation process, which is usually very hard to simulate by conventional molecular dynamics simulations. As first step, a conventional molecular dynamics simulation has been run to equilibrate the structure and the density of the solvated membrane and to evaluate its stability. The electron density through the lipid bilayer was the first property to be computed to characterize the membrane structure, and it is plotted in Figure 1B. The two peaks of the profile that appear at around -18 and 18 Å in the z axis indicate the position of the polar head groups of the lipid chains, which present heteroatoms (O, N and P) with a relatively large number of electrons, while the valley at 0 Å corresponds to the centre of the bilayer, where the electron density is lower. As can be seen in Figure 1B, the electron densities computed for the first 10 ns of the simulation and for the entire simulation time (100 ns) are virtually the same. This indicates that the lipid molecules of the bilayer do not suffer important diffusion processes along the simulation. The area per lipid, which is defined as the average area that a single lipid molecule occupies on the interface, is the second property analysed to evaluate the stability of the system. Figure 1C shows that the area per lipid oscillates around a constant value of 70.5 $Å^2$ along the 100 ns simulation, with oscillations between 69 and 72 $Å^2$ and a standard deviation of 0.73 $Å^2$. This small oscillation amplitude also corroborates the high stability of the solvated membrane and the robustness of the theoretical model employed. In addition, the small variation underwent by both the electron density and the area per lipid with

time indicates that the initial structure was already close to be equilibrated. Therefore, the solvated structure after the 100 ns molecular dynamics simulation is a good initial structure for the subsequent umbrella sampling simulations.

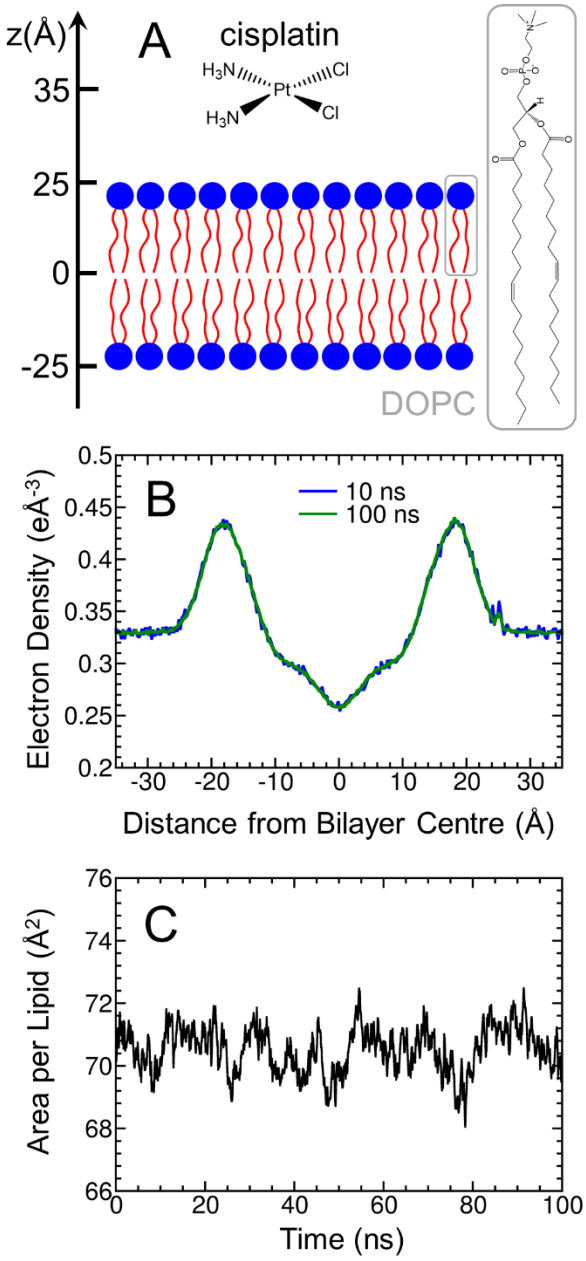

Figure 1. Analysis of the equilibration process of the DOPC membrane. (A) Schematic representation of cisplatin and the DOPC membrane. Several reference values along the z axis

are shown. (B) Electron density profile through the membrane computed for the first 10 ns (blue) and for 100 ns (green) during the equilibration molecular dynamics simulation. (C) Time evolution of the area per lipid along the equilibration.

As mentioned above, the reaction coordinate was defined as the separation between the centre of mass of cisplatin and the centre of mass of the DOPC membrane along the z axis (see Figure 1A). The initial value of the reaction coordinate was set to 34.5 Å, which corresponds to a separation of around 10 Å between cisplatin and the top of the surface of the bilayer. The reaction coordinate was divided into 69 windows separated by 0.5 Å such that the drug diffused from the bulk solvent across half of the membrane and reached the centre of the bilayer in the last window. A value of 5 kcal/(molÅ^2) was chosen as force constant for the bias potential to keep the system inside each window while allowing overlap with the neighbouring windows. It is well known that the number of windows and the force constant of the bias harmonic potential must be properly chosen to have a good overlap among the reaction-coordinate probability distributions of consecutive windows. Such a good overlap is required to obtain an accurate free-energy profile along the reaction coordinate, also called potential of mean force, from the biased probability distributions, especially when the WHAM approach is employed.[57] Figure 2A shows the computed probability distributions for the umbrella sampling windows centred at 10.0, 10.5, 11.0, 11.5 and 12.0 Å as example windows. It can be seen that the distributions of neighbouring windows present a strong overlap, which indicates a good sampling along the reaction coordinate and validates the choice of the simulation parameters employed.

Two additional important factors that determine the accuracy of the calculated free energy are the number of snapshots considered per window and the way they are chosen. When the reaction coordinate is modified to drive the system from one window to the next one, it is usually

necessary a short equilibration process in the new window such that the system accommodates to the new value of the reaction coordinate. It is advisable to compute the free-energy profile without considering those snapshots that belong to the equilibration stage. Moreover, an accurate free-energy profile is obtained only if the simulation in each window has been run for sufficient time. These two important issues are discussed in the following analysis. Figure 2B displays the potential of mean force computed for the whole simulation time (15 ns per window) and for different time intervals where the initial steps of each window were not considered; specifically, the initial 1, 2, 3, 4 and 5 ns were removed from the analysis. Note that in the profile plotted in Figure 2B the reactants (cisplatin in the bulk solvent) and the products (cisplatin integrated inside the bilayer) are located on the right and on the left side of the plot, respectively. Therefore, the uptake of cisplatin in the membrane occurs from right to left. As can be seen in the inset of Figure 2B, it is necessary to eliminate the first 2 ns of simulation to obtain a converged profile around the free-energy minimum located at 26 Å and the maximum located at 20 Å. Therefore, in this case, the system adapts to the new reaction coordinate value when it migrates from one window to the next one only after 2 ns are elapsed. However, just to be on the safe side, in the subsequent analyses the first 3 ns of each window will not be considered. Next, we analyse for how long each window must be evolved to get a converged free-energy profile. Figure 2C shows that convergence is achieved after running 8 ns (from 3 ns to 11 ns) of dynamics simulation per window. Therefore, it is not necessary to extend the simulations for longer time than the 15 ns per window initially run. The energetic analysis discussed below will be performed by taking into account snapshots from the time interval from 3 to 15 ns in each window.

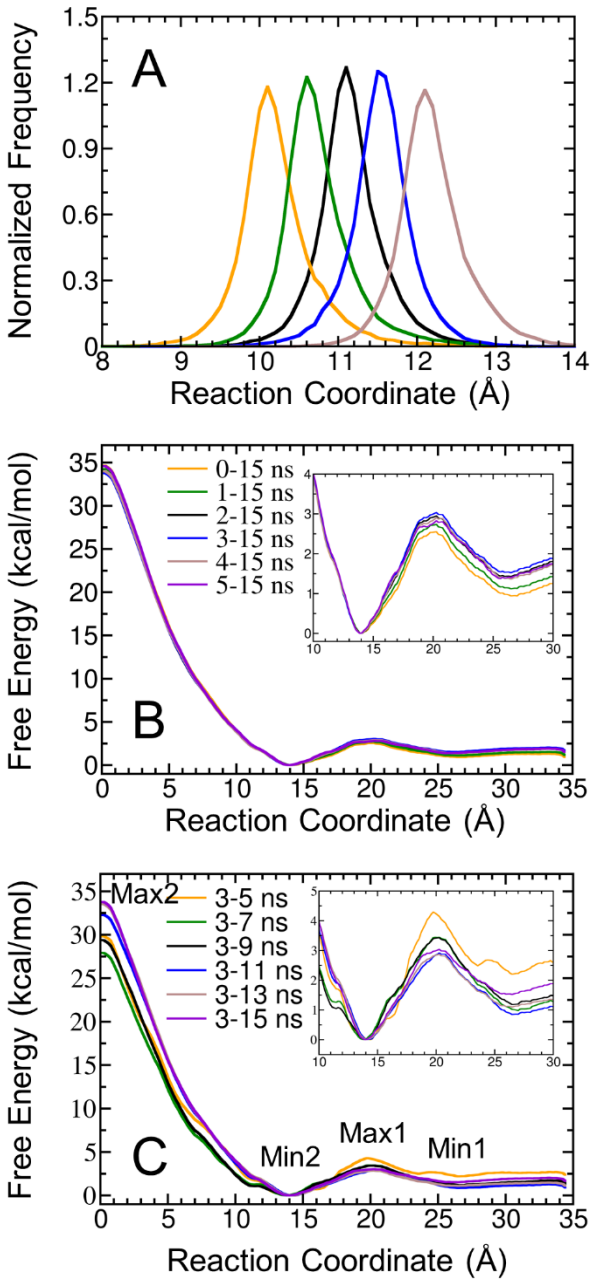

Figure 2. Convergence analysis of the umbrella sampling simulations. (A) Reaction coordinate probability distributions for the windows centered at 10.0, 10.5, 11.0, 11.5 and 12.0 Å. (B) Potential of mean force computed by removing different time intervals from the beginning of each window. (C) Potential of mean force computed for different computational times from the initial time of 3 ns.

Characterization of Intermolecular Interactions

The potential of mean force presents two energy minima and two energy maxima – called Min1, Min2, Max1 and Max2 in Figure 2C – that will be analysed in detail in the following. When cisplatin approaches the membrane, there is an initial attraction between the drug and the bilayer which results in a free-energy minimum (Min1) at 26 Å of 0.5 kcal/mol depth with respect to the energy of cisplatin located in the bulk solvent. This free-energy minimum corresponds to a weak physisorption of cisplatin on the top of the membrane. Then, a deeper minimum (Min2) at 14 Å is reached after overcoming a free-energy barrier (Max1) of 1.5 kcal/mol located at 20 Å. This second minimum is 1.5 kcal/mol lower in energy than the first one, indicating that cisplatin is more stabilized at Min2. If cisplatin continues the diffusion pathway towards the centre of the bilayer the free energy steadily increases until achieving its absolute maximum (Max2) in the middle of the membrane, which is 34 kcal/mol higher than the energy of the global minimum Min2. This energy barrier is higher than expected for a molecule which is capable of diffusing through lipid bilayers. This suggests that the interactions between the drug and the nonpolar tails could be wrongly described by the force field employed here. This will be discussed in more detail below.

A visual inspection of the umbrella sampling windows located at the two minima Min1 and Min2 reveals that the environment and the behaviour of cisplatin is completely different in both minima. While cisplatin is located at the water/membrane interface at Min1 (Figure 3A), it is completely inside the polar region of the bilayer formed by the phosphocholine (PC) groups at Min2 (Figure 3B). This situation results in a higher mobility and a shorter interaction time with the lipids when the drug is located at the more external minimum Min1 than when it is at Min2. To illustrate this, we show in Figure 3C,D the time evolution of the number of interatomic

contacts between cisplatin and the lipid residue that presents the highest interaction energy with the drug, which in both minima corresponds to PC residues (PC175 for Min1 and PC223 for Min2). A contact between a cisplatin atom and a lipid atom is arbitrarily considered when the separation between both atoms is lower than 5 Å. As can be seen, interatomic contacts between cisplatin and PC175 are present only during the last 2.5 ns of the simulation in the umbrella sampling window corresponding to Min1. This means that the rest of the time cisplatin is located at other positions interacting with different lipid residues. On the contrary, the interaction between cisplatin and PC223 exists almost along the entire time window corresponding to Min2, which indicates that the motion of the drug is restrained to a small region of the bilayer surrounding PC223. Moreover, the fact that Min2 is deeper than Min1 points out that the diffusion of the drug from water to the polar region of the bilayer is thermodynamically favourable and that the attractive interactions with the PC heads are stronger than those with the solvent.

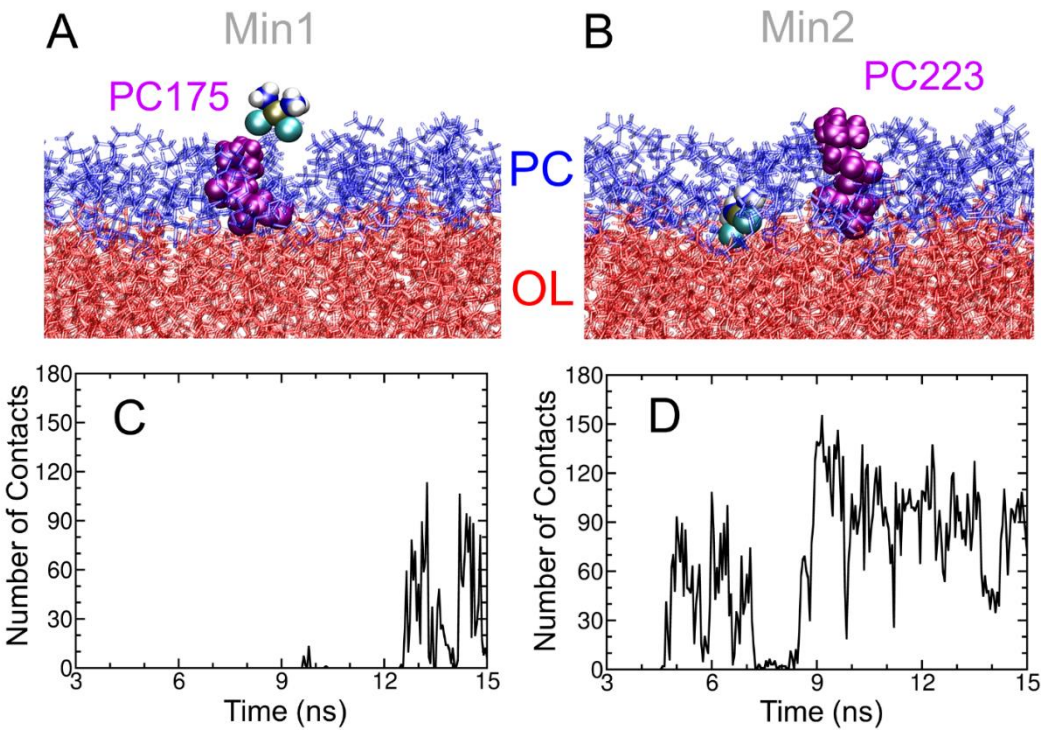

Figure 3. Analysis of the two free-energy minima Min1 and Min2. Representative snapshot of cisplatin interacting with the residue PC175 at Min1 (A) and with the residue PC223 at Min2 (B). Cisplatin is represented with van der Waals spheres with the following atom color code: ochre for Pt, blue for N, white for H and cyan for Cl. The residues PC175 and PC223 are represented by magenta van der Waals spheres. The polar heads (PC) and the nonpolar tails (OL) of the membrane are represented by blue and red sticks, respectively. Time evolution of the number of contacts between cisplatin and the residue PC175 at Min1 (C) and the residue PC223 at Min2 (D).

To get more insight on the nature of the intermolecular interactions that drive the diffusion of cisplatin through the lipid bilayer the interaction potential energy between cisplatin and the membrane was decomposed into different contributions along the permeation pathway. First, we analyze the contribution of the polar PC heads and nonpolar dioleoyl (OL) tails to the total interaction energy. The different chemical groups that belong to these two regions of the lipid chains are shown in Figure 4A. In addition, each of these contributions (PC heads and OL tails) can be further decomposed into van der Waals and electrostatic interactions, which in the force field employed here are described by Lennard-Jones and Coulomb potentials, respectively. As seen in Figure 4B,C the interaction energy between cisplatin and the PC head groups dominates along the entire reaction coordinate over the interaction between cisplatin and the OL tails, except in the region of the absolute energy maximum (Max2), where both PC and OL contributions to the total energy are similar.

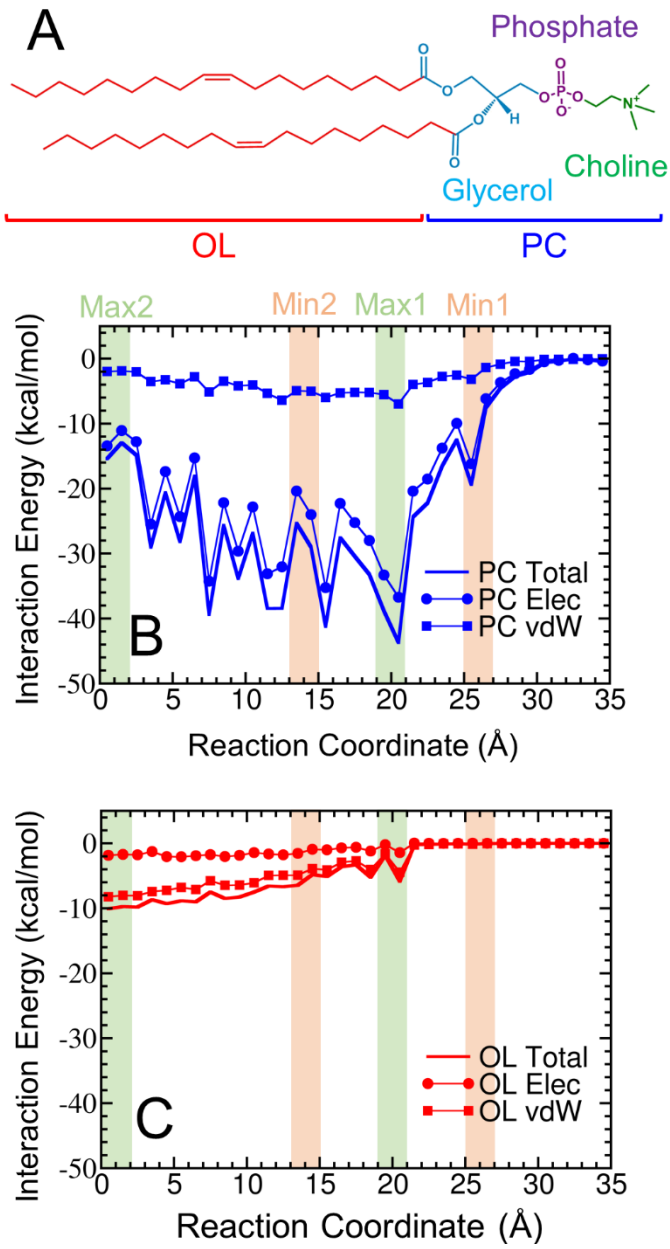

Figure 4. Contribution of phosphocholine (PC) head groups and dioleoyl (OL) tails to the cisplatin/membrane interaction energy along the reaction coordinate. (A) Different chemical groups of the DOPC lipid chains. (B) Interaction energy between cisplatin and the PC groups, and decomposition into electrostatic (Elec) and van der Waals (vdW) contributions. (C) Interaction energy between cisplatin and the OL groups, and decomposition into electrostatic (Elec) and van der Waals (vdW) contributions.

The cisplatin/PC interaction energy steadily increases (in absolute value) along the permeation pathway until the drug reaches the absolute minimum (Min2), where the attractive interaction between the drug and the head groups achieves a value around -40 kcal/mol. Then, along the pathway from Min2 to Max2, the cisplatin/PC interaction becomes less attractive until it reaches a value between -15 and -10 kcal/mol in the middle of the bilayer. Figure 4B also shows that the interaction between the drug and the polar heads is clearly dominated by electrostatic interactions, which represent 84% of the cisplatin/PC interaction energy (as average along the entire permeation pathway), while the van der Waals contribution represents only 16%.

The absolute value of the cisplatin/OL interaction energy continuously increases when the drug diffuses from the bulk solvent to the middle of the membrane, where it reaches a value of around -10 kcal/mol. Contrary to the cisplatin/PC energy, the most important contribution to the interaction between cisplatin and the nonpolar tails is given by the van der Waals interactions, which constitute 81% of the total energy. Since the cisplatin/OL attraction steadily increases along the diffusion pathway, but the cisplatin/PC attraction first increases until Min2, and then decreases from Min2 to Max2, the first half of the permeation pathway is regulated by electrostatic interactions, while in the second half of the pathway van der Waals interactions gain relevance. Specifically, the van der Waals interaction represents only 25% of the total interaction energy at the umbrella sampling window that corresponds to Min2, while it is 40% of the total energy at Max2. Such an increase of the van der Waals contribution – and the consequent drop of the electrostatic component – may have important consequences in the accuracy of the theoretical model employed.

Usually, fixed point-charge force fields, as the one used here, provide accurate results when modeling systems and processes that are largely dominated by electrostatic interactions.

However, when non-pairwise interactions, such as exchange-repulsion, polarization, and dispersion, become important it is necessary to include additional terms, *e.g.*, polarizable terms, in the force field able to describe the deformation of the electronic structure of the different molecules. Therefore, in these situations dominated by non-electrostatic interactions the use of fixed point-charge force fields may fail. We have seen in the previous analysis that the interaction energy between cisplatin and the bilayer is largely controlled by electrostatic interactions along the first half of the permeation pathway. Therefore, the force field is likely providing reliable results within this region. However, in the second half of the permeation pathway, where cisplatin is integrated into the nonpolar region of the bilayer, electrostatic interactions decrease while van der Waals interactions increase, and the total energy presents almost even contributions from both terms at the end of the pathway. Thus, it is very likely that the free-energy profile around the absolute maximum is not well described by the force field. In fact, our simulations predict an energy barrier of 34 kcal/mol for going from Min2 to Max2. If this were the case, cisplatin would be able to diffuse through lipid bilayers only in a very long-time scale of several years; and, obviously, this is not the case. Previous molecular dynamics simulations using a different fixed point-charge force field have provided an energy barrier for the cisplatin diffusion through a DOPC membrane of around 10 kcal/mol,[16, 58] which is a more reliable value. However, those simulations did not show a clear free-energy minimum on the polar region of the bilayer associated with an initial physisorption process, which is likely the first step of the permeation pathway due to the neutral charge of the drug, but an uphill pathway from the solvent to the middle of the membrane. Therefore, it seems that the simultaneous correct description of the electrostatic interactions with the polar heads and the non-electrostatic interactions with non-polar tails is very challenging for a fixed point-charge force field. The

development of a polarizable force field is likely required to accurately describe the full permeation pathway.

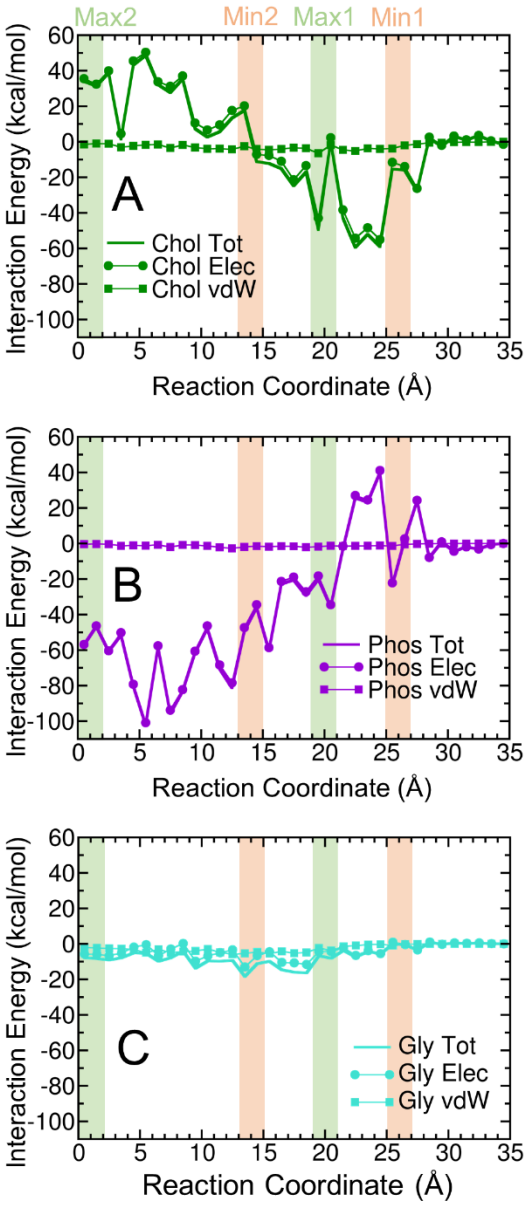

Figure 5. Decomposition of the interaction energy between cisplatin and phosphocholine (PC) groups. Interaction energy between cisplatin and the choline (A), phosphate (B), and glycerol (C) groups, together with their van der Waals and electrostatic energies decomposition, along the permeation pathway.

Since the PC heads are formed by different chemical groups, namely choline, phosphate, and glycerol groups (see Figure 4A), it is interesting to evaluate the contribution of each of these moieties to the cisplatin/PC interaction energy along the reaction coordinate and, especially, around the Min1-Max1-Min2 free-energy curve region, where the initial physisorption process occurs. Such an energy decomposition is displayed in Figure 5. Although this energy analysis contains some noise, clear trends can still be extracted. As can be seen, the glycerol groups play an almost irrelevant role along the entire reaction pathway in comparison to the choline and phosphate groups. For these last two groups, the electrostatic interactions with cisplatin largely surpass the van der Waals ones, as was already evidenced when discussing the interaction energy of the entire PC head (Figure 4B). When cisplatin is initially trapped on the top of the membrane around the region from Min1 to Max1, the attraction with the choline groups counteracts the repulsion with the phosphate units, stabilizing the system. Then, when the drug moves deeper in the bilayer, *i.e.*, from Max1 to the end of the diffusion pathway going through the Min2 minimum, the cisplatin/choline repulsion and the cisplatin/phosphate attraction steadily increase. At the global minimum Min2, the attractive interactions between cisplatin and the phosphate groups clearly dominate the system. Therefore, it can be stated that the electrostatic attractive interactions between cisplatin and choline drive the initial approach of the drug to the bilayer and, then, the electrostatic attraction with the phosphate moieties is responsible for the deeper integration of cisplatin in the absolute free-energy minimum. From Min2 to Max2, the attraction exerted by the phosphate groups is partially compensated by the repulsion with the choline units, while the van der Waals interactions with the nonpolar tails gain importance, as seen on Figure 4B.

Finally, the large number of heteroatoms present in the PC heads (see Figure 4A) could lead to the formation of hydrogen bonds with cisplatin, especially at Min1 and Min2, where the electrostatic attractive interactions with the choline and phosphate moieties, respectively, are important. The occurrence of hydrogen bonding was analysed at Min1 and Min2 assuming that a hydrogen bond is formed when the distance between the hydrogen donor and the hydrogen acceptor is shorter than 3.0 Å, and the angle formed by the hydrogen donor, hydrogen, and hydrogen acceptor is larger than 135°, which are arbitrary criteria commonly used in the literature.[59, 60] At Min1, hydrogen bonds between cisplatin and the lipids lasting for more than 1% of the simulation time were not found. This behaviour agrees with the large mobility observed for cisplatin when it is located at the water/membrane interface, as was seen in Figure 3C when analysing the time evolution of the number of contacts with the lipid chains. The formation of hydrogen bonds is slightly more relevant at Min2. Specifically, hydrogen bonding formed by the interaction of the hydrogen atoms of the amino groups of cisplatin with the oxygen atoms of phosphate groups and of the carbonyl groups of the glycerol units have been identified. However, none of these hydrogen bonds has a lifetime longer than 5% of the simulation time. Therefore, one can conclude that hydrogen bonding is not relevant for the permeation of cisplatin through the DOPC membrane. Thus, the electrostatic interactions with the choline and phosphate groups that regulate the integration of cisplatin into the bilayer are of long-range character.

CONCLUSION

The intermolecular interactions between cisplatin (and other platinum-based drugs) and cell membranes play an important role on different steps of the mode of action of these anticancer drugs, including the uptake process, resistance mechanisms and initiation of apoptosis. In addition, these interactions are also relevant on the delivery of the drug from liposomal carriers of encapsulated formulations. Therefore, the investigation of the nature of the intermolecular interactions present in cisplatin/membrane systems is crucial to gain knowledge that can contribute towards the understanding of the molecular mechanism behind the mode of action of platinum drugs and towards the design of new compounds with improved properties. In this work, we have simulated the diffusion process of cisplatin trough a DOPC lipid bilayer by means of umbrella sampling molecular dynamics simulations to unveil the mechanism of permeation of cisplatin through the lipid membrane and to characterize the intermolecular interactions which regulate this mechanism.

Cisplatin is first weakly trapped on a free-energy minimum of 0.5 kcal/mol depth that corresponds to the physisorption of cisplatin at the interface between the aqueous solvent and the polar region of the membrane. At this minimum, the mobility of cisplatin is very high and the interaction with specific residues lasts for short time (less than 3 ns). This minimum is stabilized by long-range electrostatic interactions with the choline groups of the polar region of the membrane, while hydrogen bonding is negligible. Then, the drug is driven to a deeper free-energy minimum, which is 1.5 kcal/mol lower in energy than the previous minimum, by the long-range electrostatic interactions with the phosphate groups. In this minimum, which is the global one, cisplatin is more spatially restrained and the interaction with specific residues are present for a longer time. The formation of hydrogen bonds with the oxygen atoms of phosphate

groups and of the carbonyl groups of the glycerol units occurs, although the life time of these hydrogen bonds is always shorter than 5% of the simulation time and, therefore, represents a non-relevant fraction of the total interaction energy. Along the first half of the permeation pathway, which includes the two free-energy minima and the barrier of 1.5 kcal/mol between them, the interaction of cisplatin with the glycerol moieties of the polar heads and with the non-polar tails is insignificant. In addition, the more important interactions with the choline and phosphate units are largely dominated by the electrostatic component (around 85%), while the van der Waals contribution is only minor (around 15%).

Along the second half of the permeation pathway, from the global minimum to the global maximum located at the middle of the membrane, the cisplatin/choline repulsion and the cisplatin/phosphate attraction steadily increase and partially cancel each other out. This partial cancelation induces a reduction of the total interaction energy between cisplatin and the head groups. This is accompanied by an increase of the attractive interactions between cisplatin and the non-polar tails, which is dominated by the van der Waals contribution, contrary to the interaction with the polar heads. Therefore, van der Waals interactions gain importance in the non-polar region of the membrane and represent 40% of the total cisplatin/membrane interaction energy. The energy barrier that the system must overcome to reach the global maximum is 34 kcal/mol, a value which is likely an overestimation of the real free-energy barrier. The inability of the force field to provide a more accurate value for the barrier is likely related with the drop of the electrostatic interactions in the middle of the membrane, and the consequent increase of non-electrostatic interactions, which are represented in the force field employed here by simple Lennard-Jones potentials. An accurate description of non-electrostatic interactions requires the

use of more sophisticated force fields able to describe, for example, polarization effects, which are likely very important when cisplatin interacts with the non-polar tails of the bilayer.

AUTHOR INFORMATION

Corresponding Author

Juan J. Nogueira. Chemistry Department and Institute for Advanced Research in Chemistry (IADCHEM), Universidad Autónoma de Madrid, Calle Francisco Tomás y Valiente, 7, 28049 Madrid. Website: www.mobiochem.com. Email: juan.nogueira@uam.es

Funding Sources

Attraction of Talent Program 2018 of the Comunidad de Madrid, grant reference 2018-T1/BMD-10261.

ACKNOWLEDGMENT

We thank the Comunidad de Madrid for funding through the Attraction of Talent Program (Grant Ref. 2018-T1/BMD-10261). The Centro de Computación Científica (CCC) of Universidad Autónoma de Madrid is thanked for generous computational resources.

REFERENCES

[1] Rosenberg, B., Van Camp, L., and Krigas, T. (1965) Inhibition of Cell Division in Escherichia Coli by Electrolysis Products from a Platinum Electrode, *Nature 205*, 698-699.

[2] Rosenberg, B., VanCamp, L., Trosko, J. E., and Mansour, V. H. (1969) Platinum Compounds: A New Class of Potent Antitumour Agents, *Nature 222*, 385-386.

[3] Jamieson, E. R., and Lippard, S. J. (1999) Structure, Recognition, and Processing of Cisplatin-DNA Adducts, *Chem. Rev. 99*, 2467-2498.

[4] Kelland, L. (2007) The Resurgence of Platinum-Based Cancer Chemotherapy, *Nat. Rev. Cancer 7*, 573-584.

[5] Sherman, S. E., Gibson, D., Wang, A. H. J., and Lippard, S. J. (1985) X-Ray Structure of the Major Adduct of the Anticancer Drug Cisplatin with DNA: cis-[$Pt(NH_3)_2${d(pGpG)}], *Science 230*, 412-417.

[6] Takahara, P. M., Rosenzweig, A. C., Frederick, C. A., and Lippard, S. J. (1995) Crystal Structure of Double-Stranded DNA Containing the Major Adduct of the Anticancer Drug Cisplatin, *Nature 377*, 649-652.

[7] Rabik, C. A., and Dolan, M. E. (2007) Molecular Mechanisms of Resistance and Toxicity Associated with Platinating Agents, *Cancer Treat. Rev. 33*, 9-23.

[8] Legendre, F., Bas, V., Kozelka, J., and Chottard, J. C. (2000) A Complete Kinetic Study of GG Versus AG Platination Suggests that the Doubly Aquated Derivatives of Cisplatin are the Actual DNA Binding Species, *Chem. Eur. J. 6*, 2002-2010.

[9] Martinho, N., Santos, T. C. B., Florindo, H. F., and Silva, L. C. (2019) Cisplatin-Membrane Interactions and their Influence on Platinum Complexes Activity and Toxicity, *Front. Physiol. 10*, 1898.

[10] Dasari, S., and Bernard Tchounwou, P. (2014) Cisplatin in Cancer Therapy: Molecular Mechanisms of Action, *Eur. J. Pharmacol. 740*, 364-378.

[11] Makovec, T. (2019) Cisplatin and Beyond: Molecular Mechanisms of Action and Drug Resistance Development in Cancer Chemotherapy, *Radiol. Oncol. 53*, 148-158.

[12] Mantri, Y., Lippard, S. J., and Baik, M. H. (2007) Bifunctional Binding of Cisplatin to DNA: Why Does Cisplatin Form 1,2-Intrastrand Cross-Links with AG but not with GA?, *J. Am. Chem. Soc. 129*, 5023-5030.

[13] Baik, M. H., Friesner, R. A., and Lippard, S. J. (2003) Theoretical Study of Cisplatin Binding to Purine Bases: Why Does Cisplatin Prefer Guanine over Adenine?, *J. Am. Chem. Soc. 125*, 14082-14092.

[14] Raber, J., Zhu, C., and Eriksson, L. A. (2005) Theoretical Study of Cisplatin Binding to DNA: The Importance of Initial Complex Stabilization, *J. Phys. Chem. B 109*, 11006-11015.

[15] Sharma, S., Gong, P., Temple, B., Bhattacharyya, D., Dokholyan, N. V., and Chaney, S. G. (2007) Molecular Dynamic Simulations of Cisplatin- and Oxaliplatin-d(GG) Intrastand Cross-links Reveal Differences in their Conformational Dynamics, *J. Mol. Biol. 373*, 1123-1140.

[16] Rivel, T., Ramseyer, C., and Yesylevskyy, S. (2019) The Asymmetry of Plasma Membranes and their Cholesterol Content Influence the Uptake of Cisplatin, *Sci. Rep. 9*, 5627.

[17] Yesylevskyy, S., Rivel, T., and Ramseyer, C. (2019) Curvature Increases Permeability of the Plasma Membrane for Ions, Water and the Anti-Cancer Drugs Cisplatin and Gemcitabine, *Sci. Rep. 9*, 17214.
[18] Aldossary, S. A. (2019) Review on Pharmacology of Cisplatin: Clinical Use, Toxicity and Mechanism of Resistance of Cisplatin, *Biomed. Pharmacol. J. 12*, 7-15.
[19] Dilruba, S., and Kalayda, G. V. (2016) Platinum-Based Drugs: Past, Present and Future, *Cancer Chemother. Pharmacol. 77*, 1103-1124.
[20] Johnstone, T. C., Park, G. Y., and Lippard, S. J. (2014) Understanding and Improving Platinum Anticancer Drugs - Phenanthriplatin, *Anticancer Res. 34*, 471-476.
[21] Czapla-Masztafiak, J., Nogueira, J. J., Lipiec, E., Kwiatek, W. M., Wood, B. R., Deacon, G. B., Kayser, Y., Fernandes, D. L. A., Pavliuk, M. V., Szlachetko, J., González, L., and Sá, J. (2017) Direct Determination of Metal Complexes' Interaction with DNA by Atomic Telemetry and Multiscale Molecular Dynamics, *J. Phys. Chem. Lett. 8*, 805-811.
[22] Chen, Q., Yang, Y., Lin, X., Ma, W., Chen, G., Li, W., Wang, X., and Yu, Z. (2018) Platinum(IV) Prodrugs with Long Lipid Chains for Drug Delivery and Overcoming Cisplatin Resistance, *Chem. Comm. 54*, 5369-5372.
[23] Kenny, R. G., Chuah, S. W., Crawford, A., and Marmion, C. J. (2017) Platinum(IV) Prodrugs – A Step Closer to Ehrlich's Vision?, *Eur. J. Inorg. Chem. 2017*, 1596-1612.
[24] Ramachandran, S., Temple, B., Alexandrova, A. N., Chaney, S. G., and Dokholyan, N. V. (2012) Recognition of Platinum-DNA Adducts by HMGB1a, *Biochemistry 51*, 7608-7617.
[25] Veclani, D., Melchior, A., Tolazzi, M., and Cerón-Carrasco, J. P. (2018) Using Theory to Reinterpret the Kinetics of Monofunctional Platinum Anticancer Drugs: Stacking Matters, *J. Am. Chem. Soc. 140*, 14024-14027.
[26] Harrach, S., and Ciarimboli, G. (2015) Role of Transporters in the Distribution of Platinum-Based Drugs, *Frontiers in Pharmacology 6*, 85.
[27] Eljack, N. D., Ma, H. Y. M., Drucker, J., Shen, C., Hambley, T. W., New, E. J., Friedrich, T., and Clarke, R. J. (2014) Mechanisms of Cell Uptake and Toxicity of the Anticancer Drug Cisplatin, *Metallomics 6*, 2126-2133.
[28] Kozelka, J. (2009) Molecular Origin of the Sequence-Dependent Kinetics of Reactions between Cisplatin Derivatives and DNA, *Inorg. Chim. Acta 362*, 651-668.
[29] Siddik, Z. H. (2003) Cisplatin: Mode of Cytotoxic Action and Molecular Basis of Resistance, *Oncogene 22*, 7265-7279.
[30] Chen, S. H., and Chang, J. Y. (2019) New Insights into Mechanisms of Cisplatin Resistance: From Tumor Cell to Microenvironment, *Int. J. Mol. Sci. 20*, 4136.
[31] Zhang, Y., Zeng, W., Jia, F., Ye, J., Zhao, Y., Luo, Q., Zhu, Z., and Wang, F. (2020) Cisplatin-Induced Alteration on Membrane Composition of A549 Cells Revealed by ToF-SIMS, *Surf. Interface Anal. 52*, 256-263.
[32] Ramachandran, S., Quist, A. P., Kumar, S., and Lal, R. (2006) Cisplatin Nanoliposomes for Cancer Therapy: AFM and Fluorescence Imaging of Cisplatin Encapsulation, Stability, Cellular Uptake, and Toxicity, *Langmuir 22*, 8156-8162.
[33] Rebillard, A., Tekpli, X., Meurette, O., Sergent, O., LeMoigne-Muller, G., Vernhet, L., Gorria, M., Chevanne, M., Christmann, M., Kaina, B., Counillon, L., Gulbins, E., Lagadic-Gossmann, D., and Dimanche-Boitrel, M. T. (2007) Cisplatin-Induced Apoptosis Involves Membrane Fluidification via Inhibition of NHE1 in Human Colon Cancer Cells, *Cancer Res. 67*, 7865-7874.

[34] Johnstone, T. C., Suntharalingam, K., and Lippard, S. J. (2016) The Next Generation of Platinum Drugs: Targeted Pt(II) Agents, Nanoparticle Delivery, and Pt(IV) Prodrugs, *Chem. Rev. 116*, 3436-3486.
[35] Stathopoulos, G. P., and Boulikas, T. (2012) Lipoplatin Formulation Review Article, *J. Drug Deliv. 2012*, 581363.
[36] van Meer, G., and de Kroon, A. I. P. M. (2011) Lipid Map of the Mammalian Cell, *J. Cell Sci. 124*, 5-8.
[37] Jo, S., Kim, T., Iyer, V. G., and Im, W. (2008) CHARMM-GUI: A Web-Based Graphical User Interface for CHARMM, *J. Comput. Chem. 29*, 1859-1865.
[38] Case, D. A., Ben-Shalom, I. Y., Brozell, S. R., Cerutti, D. S., Cheatham III, T. E., Cruzeiro, V. W. D., Darden, T. A., Duke, R. E., Ghoreishi, D., Gilson, M. K., Gohlke, H., Goetz, A. W., Greene, D., Harris, R., Homeyer, N., Huang, Y., Izadi, S., Kovalenko, A., Kurtzman, T., Lee, T. S., LeGrand, S., Li, P., Lin, C., Liu, J., Luchko, T., Luo, R., Mermelstein, D. J., Merz, K. M., Miao, Y., Monard, G., Nguyen, C., Nguyen, H., Omelyan, I., Onufriev, A., Pan, F., Qi, R., Roe, D. R., Roitberg, A., Sagui, C., Schott-Verdugo, S., Shen, J., Simmerling, C. L., Smith, J., Salomon-Ferrer, R., Swails, J., Walker, R. C., Wang, J., Wei, H., Wolf, R. M., Wu, X., Xiao, L., York, D. M., and Kollman, P. A. (2018) AMBER 18, University of California, San Francisco.
[39] Skjevik, Å. A., Madej, B. D., Walker, R. C., and Teigen, K. (2012) LIPID11: A Modular Framework for Lipid Simulations Using Amber, *J. Phys. Chem. B 116*, 11124-11136.
[40] Dickson, C. J., Madej, B. D., Skjevik, Å. A., Betz, R. M., Teigen, K., Gould, I. R., and Walker, R. C. (2014) Lipid14: The Amber Lipid Force Field, *J. Chem. Theory Comput. 10*, 865-879.
[41] Jorgensen, W. L., Chandrasekhar, J., Madura, J. D., Impey, R. W., and Klein, M. L. (1983) Comparison of Simple Potential Functions for Simulating Liquid Water, *J. Chem. Phys. 79*, 926-935.
[42] Li, P., Song, L. F., and Merz, K. M. (2015) Systematic Parameterization of Monovalent Ions Employing the Nonbonded Model, *J. Chem. Theory Comput. 11*, 1645-1657.
[43] Li, P., and Merz, K. M. (2016) MCPB.py: A Python Based Metal Center Parameter Builder, *J. Chem. Inf. Model. 56*, 599-604.
[44] Frisch, M. J., Trucks, G. W., Schlegel, H. B., Scuseria, G. E., Robb, M. A., Cheeseman, J. R., Scalmani, G., Barone, V., Petersson, G. A., Nakatsuji, H., Li, X., Caricato, M., Marenich, A. V., Bloino, J., Janesko, B. G., Gomperts, R., Mennucci, B., Hratchian, H. P., Ortiz, J. V., Izmaylov, A. F., Sonnenberg, J. L., Williams, Ding, F., Lipparini, F., Egidi, F., Goings, J., Peng, B., Petrone, A., Henderson, T., Ranasinghe, D., Zakrzewski, V. G., Gao, J., Rega, N., Zheng, G., Liang, W., Hada, M., Ehara, M., Toyota, K., Fukuda, R., Hasegawa, J., Ishida, M., Nakajima, T., Honda, Y., Kitao, O., Nakai, H., Vreven, T., Throssell, K., Montgomery Jr., J. A., Peralta, J. E., Ogliaro, F., Bearpark, M. J., Heyd, J. J., Brothers, E. N., Kudin, K. N., Staroverov, V. N., Keith, T. A., Kobayashi, R., Normand, J., Raghavachari, K., Rendell, A. P., Burant, J. C., Iyengar, S. S., Tomasi, J., Cossi, M., Millam, J. M., Klene, M., Adamo, C., Cammi, R., Ochterski, J. W., Martin, R. L., Morokuma, K., Farkas, O., Foresman, J. B., and Fox, D. J. (2016) Gaussian 16 Rev. C.01, Wallingford, CT.
[45] Li, P., Roberts, B. P., Chakravorty, D. K., and Merz, K. M. (2013) Rational Design of Particle Mesh Ewald Compatible Lennard-Jones Parameters for +2 Metal Cations in Explicit Solvent, *J. Chem. Theory Comput. 9*, 2733-2748.

[46] Wang, J., Wolf, R. M., Caldwell, J. W., Kollman, P. A., and Case, D. A. (2004) Development and Testing of a General Amber Force Field, *J. Comput. Chem. 25*, 1157-1174.
[47] Salomon-Ferrer, R., Götz, A. W., Poole, D., Le Grand, S., and Walker, R. C. (2013) Routine Microsecond Molecular Dynamics Simulations with AMBER on GPUs. 2. Explicit Solvent Particle Mesh Ewald, *J. Chem. Theory Comput. 9*, 3878-3888.
[48] Crowley, M. F., Darden, T. A., Cheatham Iii, T. E., and Deerfield Ii, D. W. (1997) Adventures in Improving the Scaling and Accuracy of a Parallel Molecular Dynamics Program, *J. Supercomput. 11*, 255-278.
[49] Miyamoto, S., and Kollman, P. A. (1992) Settle: An Analytical Version of the SHAKE and RATTLE Algorithm for Rigid Water Models, *J. Comput. Chem. 13*, 952-962.
[50] Kumar, S., Rosenberg, J. M., Bouzida, D., Swendsen, R. H., and Kollman, P. A. (1992) The Weighted Histogram Analysis Method for Free-Energy Calculations on Biomolecules. I. The Method., *J. Comput. Chem. 13*, 1011-1021.
[51] Grossfield, A. WHAM: The Weighted Histogram Analysis Method, version 2.09, http://membrane.urmc.rochester.edu/wordpress/?page_id=126.
[52] Roe, D. R., and Cheatham, T. E. (2013) PTRAJ and CPPTRAJ: Software for Processing and Analysis of Molecular Dynamics Trajectory Data, *J. Chem. Theory Comput. 9*, 3084-3095.
[53] Humphrey, W., Dalke, A., and Schulten, K. (1996) VMD: Visual Molecular Dynamics, *J. Mol. Graphics 14*, 33-38.
[54] Nogueira, J. J., Meixner, M., Bittermann, M., and González, L. (2017) Impact of Lipid Environment on Photodamage Activation of Methylene Blue, *ChemPhotoChem 1*, 178-182.
[55] Sánchez-Murcia, P. A., Nogueira, J. J., and González, L. (2018) Exciton Localization on Ru-Based Photosensitizers Induced by Binding to Lipid Membranes, *J. Phys. Chem. Lett. 9*, 683-688.
[56] Lee, C. T., Comer, J., Herndon, C., Leung, N., Pavlova, A., Swift, R. V., Tung, C., Rowley, C. N., Amaro, R. E., Chipot, C., Wang, Y., and Gumbart, J. C. (2016) Simulation-Based Approaches for Determining Membrane Permeability of Small Compounds, *J. Chem. Inf. Model. 56*, 721-733.
[57] Kästner, J. (2011) Umbrella Sampling, *WIREs: Comput. Mol. Sci. 1*, 932-942.
[58] Yesylevskyy, S., Cardey, B., Kraszewski, S., Foley, S., Enescu, M., da Silva, A. M., Santos, H. F. D., and Ramseyer, C. (2015) Empirical Force Field for Cisplatin Based on Quantum Dynamics Data: Case Study of New Parameterization Scheme for Coordination Compounds, *J. Mol. Model. 21*, 268.
[59] De Vetta, M. D., González, L., and Nogueira, J. J. (2018) Hydrogen Bonding Regulates the Rigidity of Liposome-Encapsulated Chlorin Photosensitizers, *ChemistryOpen 7*, 475-483.
[60] Gong, Q., Zhang, H., and Chen, C. (2019) Calculating the Absolute Binding Free Energy of the Insulin Dimer in an Explicit Solvent, *RSC Adv. 10*, 790-800.